

## The KLOE-2 project at the DAΦNE accelerator upgraded in luminosity

S. FIORE(\*) on behalf of the KLOE-2 COLLABORATION

*Dipartimento di Fisica, Sapienza Università di Roma, Italy and  
INFN, Sezione di Roma - p.le Aldo Moro 2, 00185 Roma, Italy*

(ricevuto il 29 Settembre 2011; pubblicato online il 26 Gennaio 2012)

**Summary.** — The KLOE-2 experiment is going to start a new data taking campaign at the upgraded DAΦNE collider. Highlights on the main physics results of KLOE will be presented, followed by present and future detector upgrades and estimates of their impact on the physics program.

PACS 03.65.Yz – Decoherence; open systems; quantum statistical methods.

PACS 12.15.Hh – Determination of Cabibbo-Kobayashi & Maskawa (CKM) matrix elements.

PACS 13.20.-v – Leptonic, semileptonic, and radiative decays of mesons.

### 1. – Introduction

The KLOE experiment has taken data at the Frascati  $\phi$  factory DAΦNE, an  $e^+e^-$  collider running at  $\sqrt{s} \sim 1020$  MeV ( $\phi$  mass) with beams colliding with a crossing angle of  $(\pi - 0.025)$  rad. KLOE is a multipurpose detector, mainly consisting of a large cylindrical drift chamber with an inner radius of 25 cm and an outer radius of 2 m, surrounded by a lead-scintillating fibers electromagnetic calorimeter. Both are immersed in the 0.52 T field of a superconducting solenoid. Peculiar to KLOE is the spherical, 10 cm radius, beam pipe which allows  $K_S^0$  mesons produced in  $\phi$  decays to move in vacuum before decaying. Details of the detector can be found in refs. [1-5]. From 2000 to 2006, KLOE has acquired  $2.5 \text{ fb}^{-1}$  of data at the  $\phi(1020)$  peak, plus additional  $250 \text{ pb}^{-1}$  off the  $\phi$  peak, mostly at 1000 MeV.

The  $\phi$  meson predominantly decays into charged and neutral kaons, thus allowing KLOE to make precision studies in the fields of flavor physics and low energy QCD. The latter can also be addressed using  $\phi$  meson radiative decays into scalar or pseudoscalar particles. Test of discrete symmetries conservation can be performed using several different methods. More details can be found in ref. [6]. Some of the main KLOE physics

---

(\*) E-mail: [salvatore.fiore@roma1.infn.it](mailto:salvatore.fiore@roma1.infn.it)

results will be discussed in the following, and their possible improvements thanks to the new KLOE-2 run with detector upgrades will be discussed [7].

## 2. – CKM Unitarity and lepton universality

Purely leptonic and semileptonic decays of K mesons ( $K \rightarrow \ell\nu$ ,  $K \rightarrow \pi\ell\nu$ ,  $\ell = e, \mu$ ) are mediated in the Standard Model (SM) by tree-level W-boson exchange. Gauge coupling universality and three-generation quark mixing imply that semileptonic processes such as  $d^i \rightarrow u^j \ell \nu$  are governed by the effective Fermi constant  $G_{ij} = G_\mu V_{ij}$ , where  $G_\mu$  is the muon decay constant, and  $V_{ij}$  are the elements of the unitary Cabibbo-Kobayashi Maskawa (CKM) matrix. This implies the universality relations: i) in the SM the effective semileptonic constant  $G_{ij}$  does not depend on the lepton flavor (*lepton universality*); ii) if one extracts  $V_{ij}$  from different semileptonic transitions assuming quark-lepton gauge universality (*i.e.* normalizing the decay rates with  $G_\mu$ ), the CKM unitarity condition  $\sum_j |V_{ij}|^2 = 1$  should be verified.

Precision tests of the universality relations probe physics beyond the SM and are sensitive to several SM extensions [8-11]. After four years of data analysis, KLOE has produced the most comprehensive set of results from a single experiment, measuring the main BRs of  $K_L$  [12],  $K^\pm$  [13-15] and  $K_S$  [16, 17] (unique to KLOE), including semileptonic and two-body decays; lifetime measurements for  $K_L$  [18] and  $K^\pm$  [19]; form factor slopes from the analysis of  $K_L e 3$  [20] and  $K_L \mu 3$  [21, 22]. A value of  $|V_{us}| \times f_+(0) = 0.2157(6)$  has been obtained [23] using the  $K_S$  lifetime from PDG [24] as the only non-KLOE input, since at that time the new KLOE measurement of  $K_S$  lifetime [25] was not published. This result is compatible with the world-averaged value, with the same precision. These data together with the value of  $|V_{us}|/|V_{ud}|$  from the KLOE measurement of the  $K^\pm \rightarrow \mu^\pm \nu(\gamma)$  branching ratio [14] and the extraction of  $|V_{ud}|$  from superallowed nuclear  $\beta$  decays, provide the basis for testing the unitarity of the quark-flavor mixing matrix:  $1 - |V_{ud}|^2 - |V_{us}|^2 = 9(8) \times 10^{-4}$  [23]. Both more statistics and improvements on signal selection are needed to improve the related lifetimes and branching ratios measurements, and reach better sensitivity on unitarity tests.

## 3. – CPT symmetry and quantum mechanics

A unique feature of the  $\phi$ -factory is the production of neutral kaon pairs in a pure quantum state. This state exhibits maximal entanglement which has been observed in the  $\phi \rightarrow K_S K_L \rightarrow \pi^+ \pi^- \pi^+ \pi^-$  [26] by the KLOE collaboration in year 2005. Since then, more data (a total of  $1.7 \text{ fb}^{-1}$ ) and improvements in the analysis procedure have brought to the results on several decoherence and *CPT*-violating parameters. Different hypotheses on decoherence and *CPT*-violating phenomena are expressed by different modifications of the function:

$$I(\pi^+ \pi^-, \pi^+ \pi^-; \Delta t) \propto e^{-\Gamma_L \Delta t} + e^{-\Gamma_S \Delta t} - 2e^{-\frac{(\Gamma_S + \Gamma_L)}{2} \Delta t} \cos(\Delta m \Delta t),$$

where  $\Delta t$  is the absolute value of the time difference of the two  $\pi^+ \pi^-$  decays. The modified expressions have been then used to obtain the best values of the QM- and *CPT*-violating parameters ( $\zeta_{K_S K_L}$ ,  $\zeta_{K^0 \bar{K}^0}$ ,  $\gamma$ ,  $\Re\omega$ ,  $\Im\omega$ ,  $\Delta a_X$ ,  $\Delta a_Y$ ,  $\Delta a_Z$ ) [26, 27]. In general all decoherence effects show a deviation from the quantum mechanical prediction  $I(\pi^+ \pi^-, \pi^+ \pi^-; \Delta t = 0) = 0$ . Hence the reconstruction of events in the region  $\Delta t \approx 0$ ,

*i.e.*, with vertices close to the IP, is crucial for precise determination of the parameters related to  $CPT$  violation and to decoherence.

#### 4. – Low-energy QCD

**4'1.  $K_S \rightarrow \gamma\gamma$ .** – A precise measurement of the  $K_S \rightarrow \gamma\gamma$  decay rate is an important test of Chiral Perturbation Theory (ChPT) predictions. The decay amplitude of  $K_S \rightarrow \gamma\gamma$  has been evaluated at leading order of ChPT [28],  $\mathcal{O}(p^4)$ , providing a precise estimate of  $\mathcal{B}(K_S \rightarrow \gamma\gamma) = 2.1 \times 10^{-6}$ , with 3% uncertainty. This estimate is  $\sim 30\%$  lower with respect to the latest determination from NA48 [29], thus suggesting relevant contributions from higher order corrections. KLOE measured the  $K_S \rightarrow \gamma\gamma$  rate using  $1.9 \text{ fb}^{-1}$  of integrated luminosity, obtaining [30]

$$(1) \quad \mathcal{B}(K_S \rightarrow \gamma\gamma) = (2.26 \pm 0.12_{\text{stat}} \pm 0.06_{\text{syst}}) \times 10^{-6},$$

which differs by  $3\sigma$  from the previous best determination. Our result is also consistent with  $\mathcal{O}(p^4)$  ChPT prediction. The background composition is dominated by  $K_S \rightarrow 2\pi^0$ , with two photons pointing the beam pipe region being undetected by the EMC.

**4'2.  $\eta$  pseudoscalar meson.** –  $CP$  violation in flavor-conserving processes can be tested in the  $\eta$  decays to final states that are, as in the  $K_L$  case:  $\eta \rightarrow \pi\pi$ ,  $\eta \rightarrow \pi^0 e^+ e^-$  and  $\eta \rightarrow \pi^+ \pi^- e^+ e^-$  decay. In the latter,  $CP$  violation could manifest in the angular asymmetry between the  $\pi^+ \pi^-$  and  $e^+ e^-$  decay planes. The  $\eta \rightarrow \pi^+ \pi^- e^+ e^-$  decay has been studied with KLOE [31], which measured an asymmetry  $A_\phi$  in the angle between the  $\pi\pi$  and  $ee$  decay planes consistent with zero with 3% accuracy, while theoretical predictions allow this quantity to be up to 2%. The largest contribution to the uncertainty of this measurement comes from the statistical error.

#### 5. – $\gamma\gamma$ physics: a challenge for KLOE-2

The term “ $\gamma\gamma$  physics” (or “two-photon physics”) stands for the study of the reaction

$$e^+ e^- \rightarrow e^+ e^- \gamma^* \gamma^* \rightarrow e^+ e^- + X,$$

where  $X$  is some arbitrary final state with  $J^{PC} = 0^{\pm+}, 2^{\pm+}$ , not directly coupled to one photon ( $J^{PC} = 1^{--}$ ) [32]. The cross section of these processes, of  $\mathcal{O}(\alpha^4)$ , depends on the logarithm of the center of mass energy  $\sqrt{s}$ , so that, for  $\sqrt{s}$  greater than a few GeV they dominate hadronic production at  $e^+ e^-$  colliders. The cross section  $\sigma(\gamma\gamma \rightarrow X)$  was studied at  $e^+ e^-$  colliders, from PETRA to CESR to LEP, over the years. However, the experimental situation in the low-energy region,  $m_\pi \leq W_{\gamma\gamma} \leq 700 \text{ MeV}$ , [33] is unsatisfactory since it is affected by large statistical and systematic uncertainties, due to small data samples and large background contributions, very small detection efficiency and particle identification ambiguities for low-mass hadronic systems. Recently the KLOE collaboration started  $\gamma\gamma$  physics analysis, using its off-peak data sample. In fact, a huge source of background while running on the peak of the  $\phi$  resonance, comes from  $\phi$  decays, so that we need to perform background suppression adding the information coming from a tagger system with an efficient detection of scattered electrons. Figure 1 shows the flux function multiplied by an integrated luminosity  $L_{ee} = 1 \text{ fb}^{-1}$ , as a function of the  $\gamma\gamma$  invariant mass for three different center-of-mass energies. This plot demonstrates

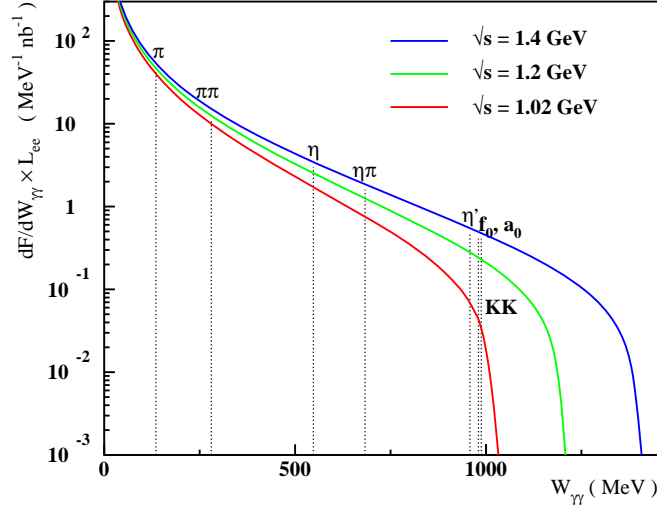


Fig. 1. – Differential  $\gamma\gamma$  flux function as a function of the center-of-mass energy.

the feasibility of the detection of the final states  $\pi^+\pi^-$ ,  $\pi^0\pi^0$ ,  $\pi^0\eta$  whose cross-sections are of the order of or larger than 1 nb [34–38], and the identification of the resonances produced in these channels, among which the controversial  $\sigma$  meson. Single pseudoscalar ( $X = \pi^0$ ,  $\eta$  or  $\eta'$ ) production is also accessible and would improve the determination of the two-photon decay widths of these mesons, relevant for the measurement of the transition form factors  $\mathcal{F}_{X\gamma^*\gamma^*}(q_1^2, q_2^2)$  as a function of the momentum of the virtual photons,  $q_1^2$  and  $q_2^2$ . The interest in such form factors is rising in connection with the theoretical evaluation of the hadronic light-by-light contribution to the muon magnetic anomaly.

## 6. – KLOE-2 detector upgrades

During year 2008 the Accelerator Division of the Frascati Laboratory has tested a new interaction scheme on the DAΦNE  $\phi$ -factory collider, with the goal of reaching a peak luminosity of  $5 \times 10^{32} \text{ cm}^{-2} \text{ s}^{-1}$ , a factor of three larger than what previously obtained. The test has been successful [39,40], and the commissioning of DAΦNE for the approved KLOE-2 run [41] has started in 2011. For this new run [42], upgrades have also been proposed and realized for the detector.

A tagging system has been installed along the beam line to detect the scattered electrons/positrons from  $\gamma\gamma$  interactions. The electron tagger is essential to study  $\gamma\gamma$  physics while running at  $\sqrt{s} = M_\phi$ , in order to reduce the large background from  $\phi$  decays. Leptons from  $\gamma\gamma$  interactions, with  $E < 510 \text{ MeV}$ , follow a path through the machine optics different from the orbit of the circulating beams. For this reason we have built two different detectors in different regions on both sides of the interaction point (IP): the Low Energy Tagger (LET) to detect leptons with energy between 150 and 400 MeV and the High Energy Tagger (HET) for those with energy greater than 420 MeV.

The LET region is one meter from the IP, inside the KLOE-2 magnetic field. In this region the correlation between the energy and the position of the leptons is weak. For this reason the LET detector is made by two LYSO crystal calorimeters, read out by Silicon Photomultipliers able to measure the electron/positron energy with a resolution

better than 10% over the range [150–400] MeV [43]. The LET has been installed in June 2010, and after a commissioning phase is ready to take data.

The HET detector consists in a couple of hodoscopes, located just at the exit of each of the first bending dipoles after the interaction point. Each hodoscope is made of plastic scintillators read out by photomultipliers [44]. In this position the off-momentum electrons or positrons escaping from the beam-pipe show a clear correlation between energy and deviation from the nominal orbit. Therefore the energy of the particles can be obtained from the measurement of the displacement with respect to the machine orbit using a position detector. The beam pipe has been modified on this purpose and is ready to host two HET stations, which are going to be installed before the end of 2011.

In a second phase, three additional detectors will be added to KLOE-2. A light-material internal tracker (IT) will be installed in the region between the beam pipe and the drift chamber inner wall to improve charged vertex resolution by a factor  $\approx 3$ , and to increase the acceptance for low  $p_T$  tracks [45]. It will be made of four coaxial cylindrical layers, each of them being a Triple-GEM foil detector. This allows the detector to have a total thickness of 0.015 radiation lengths. The IT will be the first cylindrical GEM detector ever built, and required a long dedicated R&D study [46]. Crystal calorimeters (CCALT) will cover the low  $\theta$ -angle region, aiming at increasing acceptance for very forward electrons and photons down to  $8^\circ$ . These calorimeters will be made of LYSO crystals read out by Silicon Photomultipliers, exploiting the technological development already done for the LET [47]. A new tile calorimeter (QCALT) will be used to instrument the DAΦNE focusing system for the detection of photons coming from  $K_L$  decays in the drift chamber. This calorimeter will cover the beam pipe and quadrupoles with a sampling structure of Tungsten and scintillating tiles [48]. Implementation of the second phase is planned for the year 2012. The total integrated luminosity collected by KLOE-2 at the end of the two phases, from here on referred as step-0 and step-1, will be  $5 \text{ fb}^{-1}$  and  $20 \text{ fb}^{-1}$ , respectively.

## 7. – Improving KLOE physics results with KLOE-2

**7.1. CKM Unitarity and lepton universality.** – KLOE-2 can significantly improve the accuracy on the measurement of  $K_L$ ,  $K^\pm$  lifetimes and  $K_{Se3}$  branching ratio with respect to present world average [49] with data from KLOE-2/step-0. The present 0.23% fractional uncertainty on  $|V_{us}| \times f_+(0)$  can be reduced to 0.14% using KLOE present data set together with the KLOE-2/step-0 statistics. The world-average uncertainties on phase space integrals and  $K_L$  semileptonic BRs [49] have been used in table I to summarize the expected accuracy on  $|V_{us}| \times f_+(0)$  for each decay mode and with the contributions from branching ratio, lifetime,  $SU(2)$ -breaking and long-distance  $EM$  corrections, and phase space integral. Statistical uncertainties on the measurement of BRs and lifetimes have been obtained scaling to the total sample of  $7.5 \text{ fb}^{-1}$  of integrated luminosity available at the completion of KLOE-2/step-0. The estimate of systematic errors is rather conservative, being based on KLOE published analyses without including any improvement from the detector upgrade.

**7.2. CPT symmetry and quantum mechanics.** – As already stated, the vertex resolution for  $K_S$  decays affects the  $I(\pi^+\pi^-, \pi^+\pi^-; \Delta t)$  distribution both reducing the sensitivity of the fit and introducing systematic uncertainties, as shown in fig. 2. The improvement on vertex resolution made through the insertion of the IT will lead to an increase of the experimental sensitivity on the decoherence parameters by a factor of two.

TABLE I. – KLOE-2/step-0 prospects on  $|V_{us}| \times f_+(0)$  extracted from  $K_{l3}$  decay rates; the fractional accuracy on partial contributions from branching fraction ( $\mathcal{B}$ ), lifetime ( $\tau$ ),  $SU(2)$  and EM corrections ( $\delta$ ) and phase-space integral ( $I_{Kl}$ ) are also shown.

Mode	$\delta V_{us}  \times f_+(0)$ (%)	$\mathcal{B}$	$\tau$	$\delta$	$I_{Kl}$
$K_L e3$	0.21	0.09	0.13	0.11	0.09
$K_L \mu3$	0.25	0.10	0.13	0.11	0.15
$K_S e3$	0.33	0.30	0.03	0.11	0.09
$K^\pm e3$	0.37	0.25	0.05	0.25	0.09
$K^\pm \mu3$	0.40	0.27	0.05	0.25	0.15

**7.3.  $K_S \rightarrow \gamma\gamma$ .** – KLOE-2 will improve both sample statistics and data quality, the latter thanks to the CCALT crystal calorimeters, that will increase the rejection of  $K_S \rightarrow \pi^0\pi^0$  with photons at low polar angle. The KLOE-2 measurement can clarify the disagreement between KLOE and NA48 [50,51] and help settling the  $\mathcal{O}(p^6)$  contributions to the amplitude  $A(K_L \rightarrow \pi^0\gamma\gamma)$ , related by chiral symmetry to the  $K_S \rightarrow \gamma\gamma$  terms only [52].

**7.4.  $\eta$  pseudoscalar meson.** – The  $\eta \rightarrow \pi^+\pi^-\pi^+\pi^-$  decay plane asymmetry measurement by KLOE is limited by the statistical uncertainties. In KLOE the minimal transverse momentum of reconstructed tracks,  $P_{T_{\min}}$ , is 23 MeV. It limits the selection efficiency to  $\sim 8\%$ . The installation of the inner tracker, in the second phase of the KLOE-2 experiment, would reduce  $P_{T_{\min}}$  to 16 MeV improving at the same time the tracking resolution [31]. With a sample of  $20 \text{ fb}^{-1}$  and the acceptance increase, KLOE-2 could measure the asymmetry  $A_\phi$  with a statistical precision better than 1%.

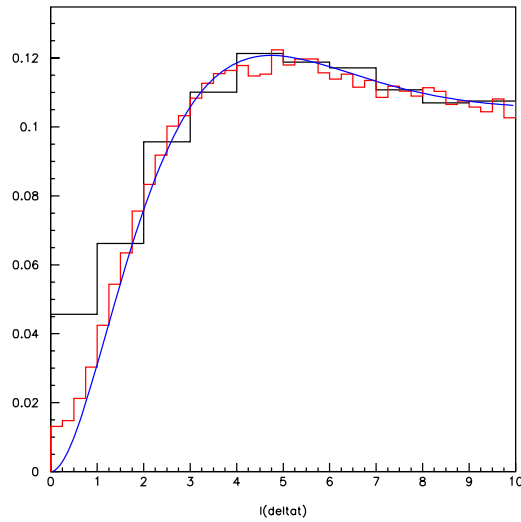


Fig. 2. – Monte Carlo simulation of the  $I(\pi^+\pi^-, \pi^+\pi^-; \Delta t)$  as a function of  $|\Delta t|$  (in  $\tau_S$  units) with the present KLOE resolution  $\sigma_{\Delta t} \approx \tau_S$  (histogram with large bins), with an improved resolution  $\sigma_{\Delta t} \approx 0.3\tau_S$  (histogram with small bins), and in the ideal case (solid line).

## REFERENCES

- [1] ADINOLFI M. *et al.*, *Nucl. Instrum. Methods A*, **488** (2002) 51.
- [2] ADINOLFI M. *et al.*, *Nucl. Instrum. Methods A*, **482** (2002) 364.
- [3] ADINOLFI M. *et al.* (KLOE COLLABORATION), *Nucl. Instrum. Methods A*, **492** (2002) 134.
- [4] ADINOLFI M. *et al.*, *Nucl. Instrum. Methods A*, **483** (2002) 649.
- [5] ALOISIO A. *et al.*, *Nucl. Instrum. Methods A*, **516** (2004) 288.
- [6] BOSSI F., DE LUCIA E., LEE-FRANZINI J., MISCETTI S. and PALUTAN M. (KLOE COLLABORATION), *Riv. Nuovo Cimento*, **31** (2008) 531, [arXiv:0811.1929](#).
- [7] AMELINO-CAMELIA G. *et al.*, *Eur. Phys. J. C*, **68** (2010) 619.
- [8] MARCIANO W. J. and SIRLIN A., *Phys. Rev. D*, **35** (1987) 1672.
- [9] HAGIWARA K., MATSUMOTO S. and YAMADA Y., *Phys. Rev. Lett.*, **75** (1995) 3605.
- [10] KURYLOV A. and RAMSEY-MUSOLF M. J., *Phys. Rev. Lett.*, **88** (2002) 071804, [hep-ph/0109222](#).
- [11] CIRIGLIANO V., JENKINS J. and GONZALEZ-ALONSO M., *Nucl. Phys. B*, **830** (2010) 95, [0908.1754](#).
- [12] AMBROSINO F. *et al.* (KLOE COLLABORATION), *Phys. Lett. B*, **632** (2006) 43, [hep-ex/0508027](#).
- [13] AMBROSINO F. *et al.* (KLOE COLLABORATION), *JHEP*, **02** (2008) 098, [arXiv:0712.3841](#).
- [14] AMBROSINO F. *et al.* (KLOE COLLABORATION), *Phys. Lett. B*, **632** (2006) 76, [hep-ex/0509045](#).
- [15] AMBROSINO F. *et al.* (KLOE COLLABORATION), *Phys. Lett. B*, **666** (2008) 305, [arXiv:0804.4577](#).
- [16] AMBROSINO F. *et al.* (KLOE COLLABORATION), *Phys. Lett. B*, **636** (2006) 173, [hep-ex/0601026](#).
- [17] AMBROSINO F. *et al.* (KLOE COLLABORATION), *Eur. Phys. J. C*, **48** (2006) 767, [hep-ex/0601025](#).
- [18] AMBROSINO F. *et al.* (KLOE COLLABORATION), *Phys. Lett. B*, **626** (2005) 15, [hep-ex/0507088](#).
- [19] AMBROSINO F. *et al.* (KLOE COLLABORATION), *JHEP*, **01** (2008) 073, [arXiv:0712.1112](#).
- [20] AMBROSINO F. *et al.* (KLOE COLLABORATION), *Phys. Lett. B*, **636** (2006) 166, [hep-ex/0601038](#).
- [21] AMBROSINO F. *et al.* (KLOE COLLABORATION), *JHEP*, **12** (2007) 105, [arXiv:0710.4470](#).
- [22] TESTA M. *et al.* (KLOE COLLABORATION) (2008), [arXiv:0805.1969](#).
- [23] AMBROSINO F. *et al.* (KLOE COLLABORATION), *JHEP*, **04** (2008) 059, [arXiv:0802.3009](#).
- [24] AMSLER C. *et al.* (PARTICLE DATA GROUP), *Phys. Lett. B*, **667** (2008) 1.
- [25] AMBROSINO F. *et al.* (KLOE COLLABORATION), *Eur. Phys. J. C*, **71** (2011) 1604.
- [26] AMBROSINO F. *et al.* (KLOE COLLABORATION), *Phys. Lett. B*, **642** (2006) 315, [hep-ex/0607027](#).
- [27] DI DOMENICO A. *et al.* (KLOE COLLABORATION), *J. Phys. Conf. Ser.*, **171** (2009) 012008.
- [28] D'AMBROSIO G. and ESPRIN D., *Phys. Lett. B*, **175** (1986) 237.
- [29] LAI A. *et al.* (NA48 COLLABORATION), *Phys. Lett. B*, **551** (2003) 7.
- [30] AMBROSINO F. *et al.* (KLOE COLLABORATION), *JHEP*, **05** (2008) 51.
- [31] AMBROSINO F. *et al.* (KLOE COLLABORATION), *Phys. Lett. B*, **675** (2009) 283, [arXiv:0812.4830](#).
- [32] PENNINGTON M. R., [arXiv:hep-ph/0511146](#) and references therein.
- [33] MARSISKE H. *et al.* (CRYSTAL BALL COLLABORATION), *Phys. Rev. D*, **41** (1990) 3324.
- [34] BOYER J. *et al.*, *Phys. Rev. D*, **42** (1990) 1350.
- [35] MARSISKE H. *et al.* (CRYSTAL BALL COLLABORATION), *Phys. Rev. D*, **41** (1990) 3324.
- [36] OEST T. *et al.* (JADE COLLABORATION), *Z. Phys. C*, **47** (1990) 343.
- [37] MORI T. *et al.* (BELLE COLLABORATION), *Phys. Rev. D*, **75** (2007) 051101, [hep-ex/0610038](#).
- [38] UEHARA S. *et al.* (BELLE COLLABORATION), *Phys. Rev. D*, **78** (2008) 052004, [arXiv:0810.0655](#).
- [39] MILARDI C. *et al.*, *ICFA Beam Dyn. Newslett.*, **48** (2009) 23.



- [40] ZOBOV M. *et al.*, *ICFA Beam Dyn. Newslett.*, **48** (2009) 34.
- [41] BECK R. *et al.* (KLOE-2 COLLABORATION) (2006), KLOE-2 Public Documents - K2PD-1, <http://www.lnf.infn.it/kloe2/>.
- [42] BECK R. *et al.* (KLOE-2 COLLABORATION) (2007), Letter of Intent for the KLOE-2 Roll-in, LNF-07/19(IR).
- [43] BABUSCI D. *et al.*, *Nucl. Instrum. Methods A*, **617** (2010) 81.
- [44] ARCHILLI F. *et al.*, *Nucl. Instrum. Methods A*, **617** (2010) 266.
- [45] ARCHILLI F. *et al.* (KLOE-2 COLLABORATION), [arXiv:1002.2572](#) (2010).
- [46] BALLA A. *et al.*, *Nucl. Instrum. Methods A*, **628** (2011) 194.
- [47] HAPPACHER F. *et al.*, *Nucl. Phys. B Proc. Suppl.*, **197** (2009) 215.
- [48] CORDELLI M. *et al.*, *Nucl. Instrum. Methods A*, **617** (2010) 105.
- [49] ANTONELLI M. *et al.* (FLAVIANET WORKING GROUP ON KAON DECAYS), [arXiv:0801.1817](#) (2008).
- [50] LAI A. *et al.* (NA48 COLLABORATION), *Phys. Lett. B*, **551** (2003) 7, [hep-ex/0210053](#).
- [51] AMBROSINO F. *et al.* (KLOE COLLABORATION), *JHEP*, **05** (2008) 051, [arXiv:0712.1744](#).
- [52] BUCHALLA G., D'AMBROSIO G. and ISIDORI G., *Nucl. Phys. B*, **672** (2003) 387, [hep-ph/0308008](#).